Development 105, 95–103 (1989)
Printed in Great Britain © The Company of Biologists Limited 1989

fushi tarazu protein expression in the cellular blastoderm of *Drosophila* detected using a novel imaging technique

TIMOTHY L. KARR* and THOMAS B. KORNBERG

Department of Biochemistry and Biophysics, University of California, San Francisco CA. 94143, USA

* Present address: Department of Biochemistry, 427 Roger Adams Laboratory, 1209 West California St., University of Illinois, Urbana, Illinois, USA

Summary

The *fushi tarazu* (*ftz*) gene is essential for segmentation of the *Drosophila* embryo. This requirement is reflected at the cellular blastoderm stage of embryogenesis by seven transverse stripes of *ftz* expression. These stripes correspond to the missing segments of *ftz* mutant embryos. We describe here novel intermediate patterns of *ftz* protein expression which were detected in younger embryos by using anti-*ftz* antibodies and a sensitive fluorescence/immunoperoxidase technique ('filtered fluorescence imaging', FFI). Striped patterns of *ftz* protein evolved continuously, and the different stripes appeared in an ordered sequence, involving both anterior–posterior (A/P) and dorsal–ventral (D/V) progressions. Comparison of these patterns of *ftz* protein with those of *ftz* RNA suggests that these novel aspects of the patterning process involve post-transcriptional regulation in addition to the transcriptional control known to be involved in expression of this gene.

Key words: pair-rule genes, segmentation, fluorescence, immunohistochemistry, *Drosophila*, *fushi tarazu*, protein expression.

Introduction

A large number of genes affecting the process of segmentation in *Drosophila* are expressed during the phase of cellularization. Extensive genetic and molecular analyses reveal a complex, and as yet incompletely understood, series of interactions among them. They are collectively referred to as segmentation genes, and patterns of larval cuticle defects observed in mutant embryos divide them into three general categories (Nüsslein-Volhard & Weischaus, 1980). Gap genes affect contiguous regions of the embryo, pair-rule genes affect alternating segment-length intervals, and segment polarity genes affect regions within each segment.

The *fushi tarazu* (*ftz*) gene was the first pair-rule gene analysed by RNA *in situ* hybridization techniques. In cellularizing embyos, it is expressed in a series of seven transverse stripes (Hafen *et al.* 1984), and these stripes of periodic expression coincide with pattern defects found in *ftz* mutant embryos (Wakimoto & Kauffman, 1981). Interestingly, nuclear cycle 10 embryos express *ftz* RNA throughout the embryo (Weir & Kornberg, 1985) but, by nuclear cycle 13, express *ftz* RNA in a restricted region spanning 15–65 % egg length (EL; 0 % EL = posterior pole). This domain of transcription resolves into the final striped pattern during nuclear cycle 14 (Hafen *et al.* 1984; Weir & Kornberg, 1985).

Using anti-*ftz* antibodies, Carroll & Scott (1985) described the appearance of seven transverse stripes of *ftz* protein in cellularizing embryos. While the precise spatial and temporal relationships between the synthesis of *ftz* RNA and protein is not yet known, major differences were observed: no protein was detected in cycle 10 embryos, or in the broad 15–65 % EL region where *ftz* RNA accumulates during cycles 12 and 13, and no protein was detected in patterns similar to the two-segment wide RNA repeat patterns seen in subsequent studies (Weir & Kornberg, 1985; Ingham *et al.* 1985). These differences raise questions concerning the control and coordination of transcription and translation of this important developmental gene.

This study describes an immunocytochemical staining technique more sensitive than standard immunoperoxidase or immunofluorescence methods. When used in conjunction with anti-*ftz* antibodies, intermediate patterns during the initial phases of *ftz* protein expression were revealed. The patterning process is characterized by the following features: (1) when first detected, stripes were wider than the mature stripes; (2) stripes appeared in the sequence: 1, 2, 3 and 5, followed by stripes 6 and 7, with stripe 4 appearing last; (3) stripes formed with a distinct dorsal–ventral polarity reminiscent of *engrailed* stripe formation (DiNardo *et al.* 1985; Weir & Kornberg, 1985); and (4) low level *ftz* ex-

pression appeared transiently in regions spanning the entire embryo.

Materials and methods

Fixation and staining of whole embryos

Whole fixed embryos were prepared essentially as described by Mitchison & Sedat (1983) with modifications as noted below. 2–4 h collections of *Drosophila* embryos were washed from corn meal/yeast agar plates with a gentle stream of NaCl/Triton rinse solution (0·9% NaCl, 0·03% Triton X-100) onto nylon mesh screen. The embryos were further washed in NaCl/Triton wash solution and then dechorionated by immersion in a 50% solution of commercial bleach for 90 seconds. Embryos were next washed thoroughly with NaCl/Triton rinse solution to remove the bleach and then fixed. The 2-phase fixative contained 5 ml of heptane, 1 ml of 37% formaldehyde (formalin solution) and 5 ml of PEM buffer (0·1 M-Pipes, 1 mM-magnesium chloride or magnesium sulphate, 1 mM-EGTA, pH 6·9) containing 1 micro-molar taxol (Karr & Alberts, 1986). However, subsequent studies have shown that similar results were obtained without taxol. Typically 200–1000 embryos were added to a 50 ml screw-top culture tube containing the 2-phase fixative and shaken at 250 revs min^{-1} on a platform shaker for 20–30 min. The vitelline membranes were removed by transferring fixed embryos into a 50/50 mixture of heptane and methanol/EGTA (prepared by the addition of 1 part 0·5 M-EGTA into 9 parts methanol) cooled to −70 °C with dry ice and vigorously shaking them on a platform shaker for 10 min. The mixture was then rapidly warmed to room temperature in a stream of hot tap water and the devitellinized embryos collected at the bottom of the vessel. The upper heptane phase was removed and the embryos washed 3 times with methanol to remove residual heptane. Before rehydration into PBST (PBS containing 0·1% Triton X-100; our PBS contained 50 mM-NaH_2PO_4, 50 mM-NaCl, 5 mM-KCl, 5 mM-$MgSO_4$, pH 7·8), embryos were treated with 3% hydrogen peroxide in 10 ml of methanol for 15 minutes to inhibit endogenous peroxidase activity.

Fluorescent and immunohistochemical staining

Immediately following the hydrogen peroxide treatment, embryos were hydrated with 3 changes of PBST and then rinsed for 30 minutes in PBST. Embryos were transferred into separate test tubes and incubated for 15 minutes in 0·5 ml of PBST containing 10% normal goat serum (GIBCO) followed by the addition of rabbit anti-*ftz* antibody to approximately 1 $\mu g\,ml^{-1}$ (kindly provided by Sean Carroll). Incubation with primary antibody typically ranged from 1 h at room temperature to overnight at 4 °C, followed by a 1–4 h rinse with three changes of PBST. Rinsed embryos were next incubated in PBS/10% normal goat serum containing a 1:100 dilution of biotinylated goat anti-rabbit antibodies (Vector labs) for 1 h, rinsed in PBST (with 3 changes) for an additional hour and then treated with a 1:100 dilution of streptavidin–horseradish peroxidase (Bethesda Research Laboratories) in 0·5 ml of PBS/10% normal goat serum for 1 h. In some experiments, we first incubated both the biotinylated rabbit antibodies and the streptavidin–horse-radish peroxidase with fixed embryos to preabsorb nonspecific binding of these reagents. It is our experience that these procedures minimize background staining, but that adequate staining can be obtained without these treatments and the individual investigator should determine the need for pre-adsorption in their own systems. Following removal of the streptavidin–horse-radish peroxidase conjugate and a 1 h rinse in three changes of PBST, histochemical colour development was initiated in 1 ml of PBST by the addition of 3,3′-diaminobenzidine to 0·1 mg ml^{-1} and hydrogen peroxide to 0·03%. The reaction can be monitored with a dissecting microscope until the desired signal is achieved, and then terminating the reaction by rinsing in PBST containing 1 mM-sodium azide. Prior to mounting under glass coverslips, nuclei were stained with the DNA-specific dye DAPI (4,6-diamidino-2-phenylindole from Sigma) at 0·1 $\mu g\,ml^{-1}$ for 5 minutes and then rinsed in PBST.

Microscopy

Embryos were prepared for microscopic examination by pipetting embryos in PBST onto slides, gently aspirating away excess buffer, additing a drop of aqueous mounting media (Flouromount G, Southern Biotechnologies), and mounting under a coverslip. All embryos were observed and photographed using a Zeiss Universal microscope equipped with bright-field, Nomarski DIC and epifluorescence optics using Zeiss ×16 or ×25 Plan-Neofluor lenses. Images were recorded on Kodak Technical Pan 2415 film and developed using Kodak HC-110 developer at dilution E.

Results

Filtered fluorescence imaging: enhanced visualization of immunostaining patterns

We have developed a filtered fluorescence imaging (FFI) technique for visualizing low level expression of nuclear antigens. Briefly, fixed embryos were treated with antibodies directed against a nuclear antigen, and bound antibody was used to localize horse-radish peroxidase (HRP) through a secondary antibody. After the bound HRP was reacted with substrate, embryos were stained with the fluorescent DNA-binding dye DAPI, and nuclei were revealed by epifluorescence microscopy. Nuclear fluorescence in regions where the antigen was present was diminished, presumably due to HRP reaction products (see Discussion).

Use of anti-*ftz* antibody with FFI generated patterns of *ftz* protein similar to those visualized previously with standard immunohistochemical techniques. However, the increased sensitivity of FFI revealed additional features. Fig. 1 shows two cellularized embryos stained with anti-*ftz* antibody. Bright-field (Fig. 1A) or Nomarski (Fig. 1D) illumination revealed seven stripes of localized *ftz* expression, in agreement with previous immunofluorescence observations (Carroll & Scott, 1985). FFI visualization (Fig. 1B,C,E, and F) not only detects these seven stripes with better contrast, but also reveals *ftz* expression in anterior and posterior regions of the embryo. There was little variability of these FFI staining patterns between embryos of similar ages, and all of the patterns were dependent upon the use of anti-*ftz* antibody and appropriate secondary antibody reagents.

Intermediate ftz *protein patterns revealed by FFI*

During cellularization, nuclei elongate and membrane furrows extend from the surface (Fullilove & Jacobson, 1971; Foe & Alberts, 1983). The large arrows in

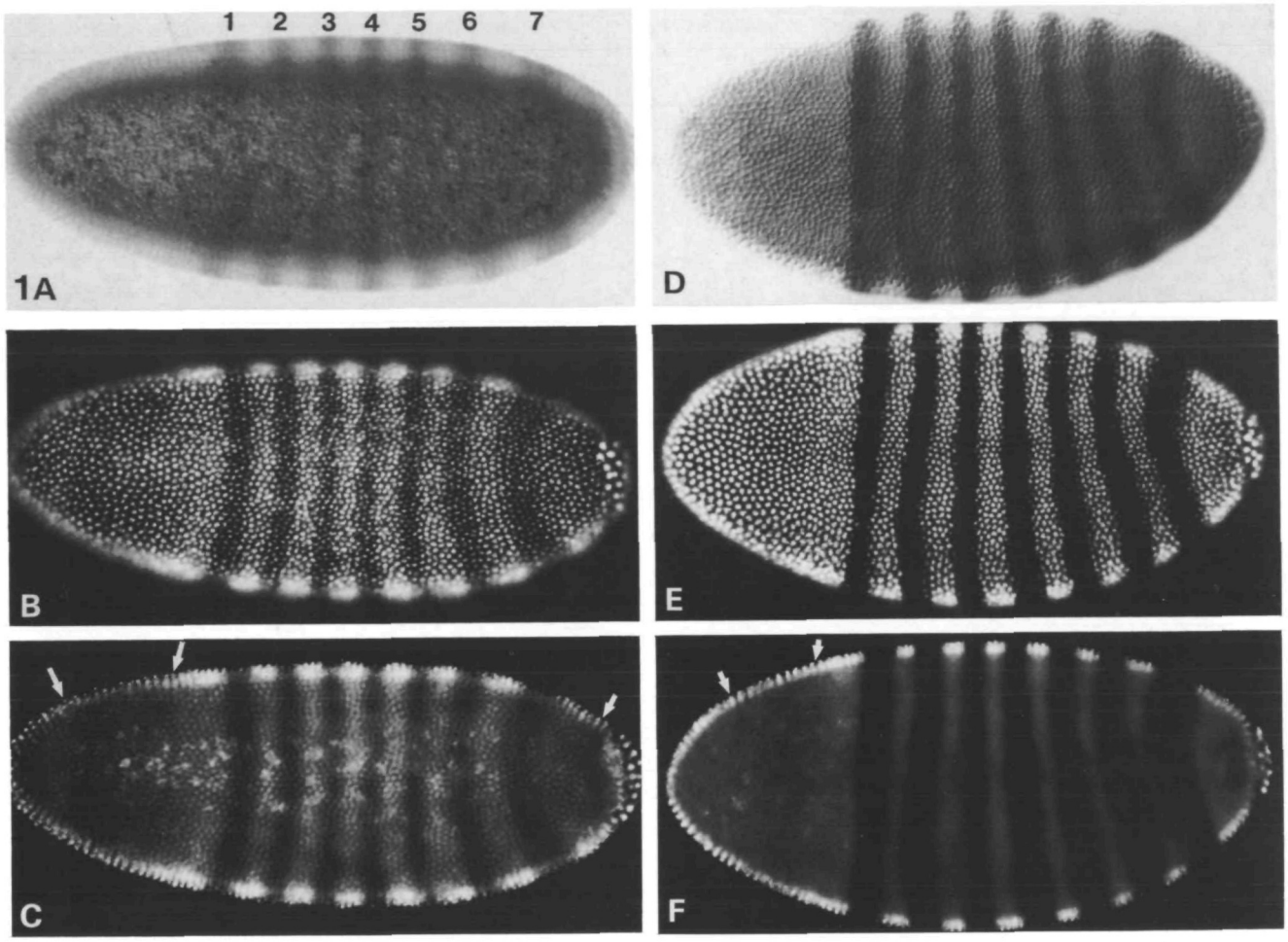

Fig. 1. *ftz* expression in late cellular blastoderm embryos. Embryos were fixed and immunoperoxidase stained as described in Methods. Nuclei were stained with the DNA-specific dye, DAPI, and viewed by bright-field (A), Nomarski DIC (D), or epifluorescence (B,C,E,F) optics. (A–C) Embryo oriented with dorsal side up, anterior left, showing the seven major stripes of *ftz* expression (numbered in A). A and C were photographed at identical focal planes (optical midsection) and B is a surface view. (D–F) Embryo oriented with ventral side up. Surface views are shown in D and E, optical midsection in F. Position of *ftz*-positive staining anterior to the central domain of seven stripes is shown by arrows in C and F. Arrow near the posterior end in C shows *ftz* expression at the posterior end of the embryo.

Fig. 2B,D, and F indicate nuclei as they change from a spherical to an elongated shape, and the small arrows in Fig. 2D and F indicate invaginating membrane furrows deepening as cellularization proceeds. These two landmark features – nuclear elongation and membrane furrowing – are excellent markers of developmental age of the fixed samples used in this study, and were used to precisely reconstruct the intermediate stages of the emerging patterns of *ftz* expression.

Continuous evolution of *ftz* protein patterns during cellularization was observed by FFI (Fig. 3). Companion bright-field images of these embryos indicate their age (Fig. 2A,C,E,G), and reveal the increased sensitivity of FFI. Stripes of *ftz* protein, identified by their position along the anterior–posterior (A/P) axis, appeared sequentially with an A/P polarity (Fig. 3A–D and Fig. 4). Inspection of the progression of stripe maturation in numerous embryos displaying staining patterns similar to those in Figs 3 and 4 indicates a consistent sequence.

Initially, broad regions of staining were observed in three areas that will produce stripes 1, 2+3, and 5+6+7 (Fig. 3A,B). However, there was no apparent temporal correlation between these broad areas and their resolution as mature stripes. The actual order of appearance of stripes was: stripes 1 and 2, followed by stripes 5 and 3, and finally stripes 6, 7, and 4 were the last to form. This progression is summarized in Fig. 5.

Maturation of the striped pattern

Several aspects of the stripes changed as they matured. First, stripes 3–7 had a graded D/V distribution (Fig. 3E,F and Fig. 4). Staining was most intense on the ventral side, gradually tapering off towards the dorsal midline. Stripes 1 and 2 generally had less graded expression. Second, the stripes narrowed with time. FFI revealed that stripes of *ftz* protein were wider in the intermediate stages than in their mature form. For

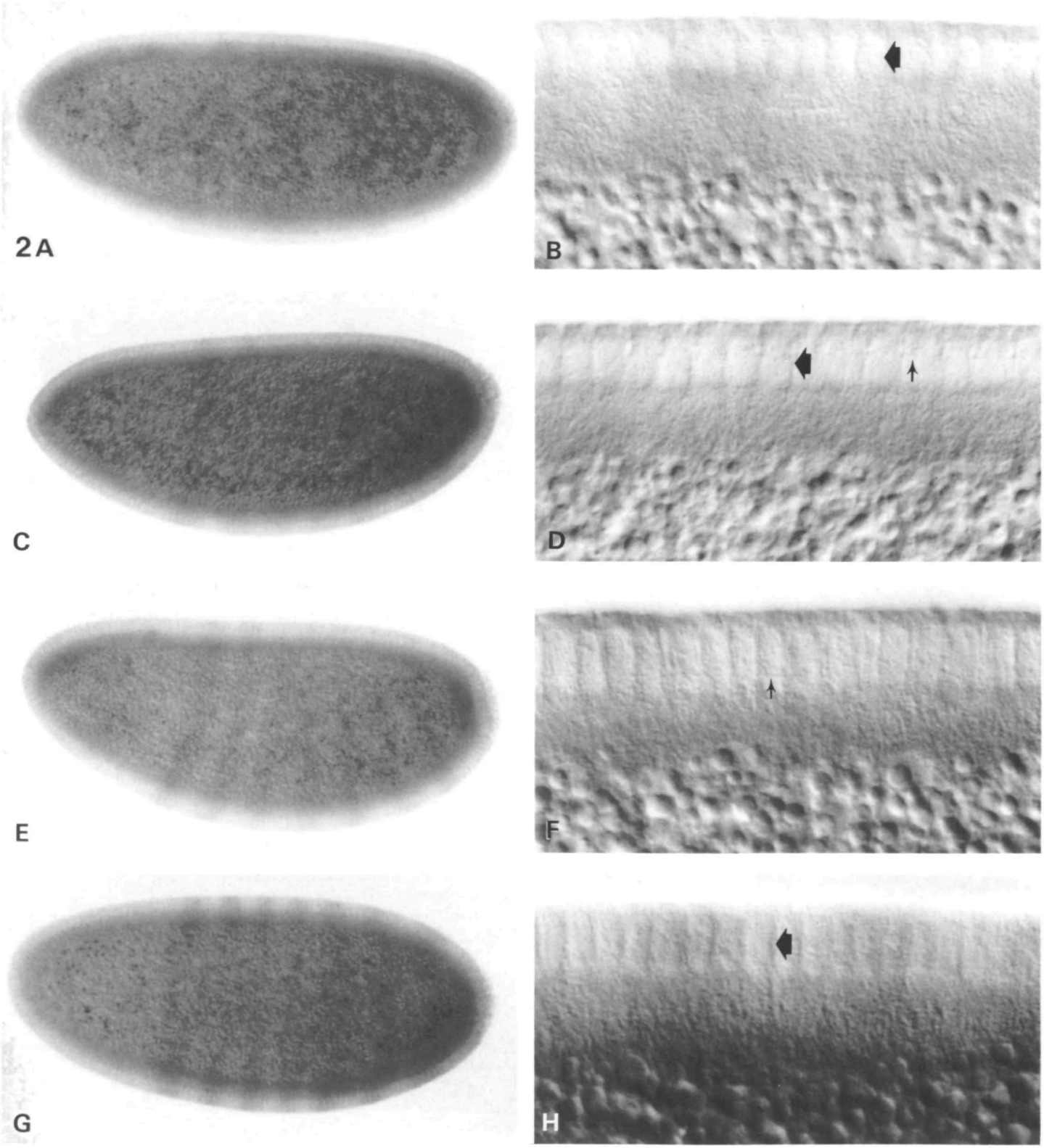

Fig. 2. *ftz* expression in cellularizing embryos – immunoperoxidase stain. Four embryos fixed during various stages of cellularization and immunoperoxidase stained using anti-*ftz* antibodies are shown. On the left are bright-field images (A,C,E,G) of successive stages of cellularization as determined by high-magnification observation (B,D,F,H) of the extent of cellularization using Nomarski DIC optics. The landmark features used to follow cellularization are nuclear shape changes (large arrows in B,D and H) and the advancement of the invaginating membrane (small arrows in D and F). The first three embryos are lateral views, oriented anterior to the left and dorsal side up except G which is viewed with the dorsal side up.

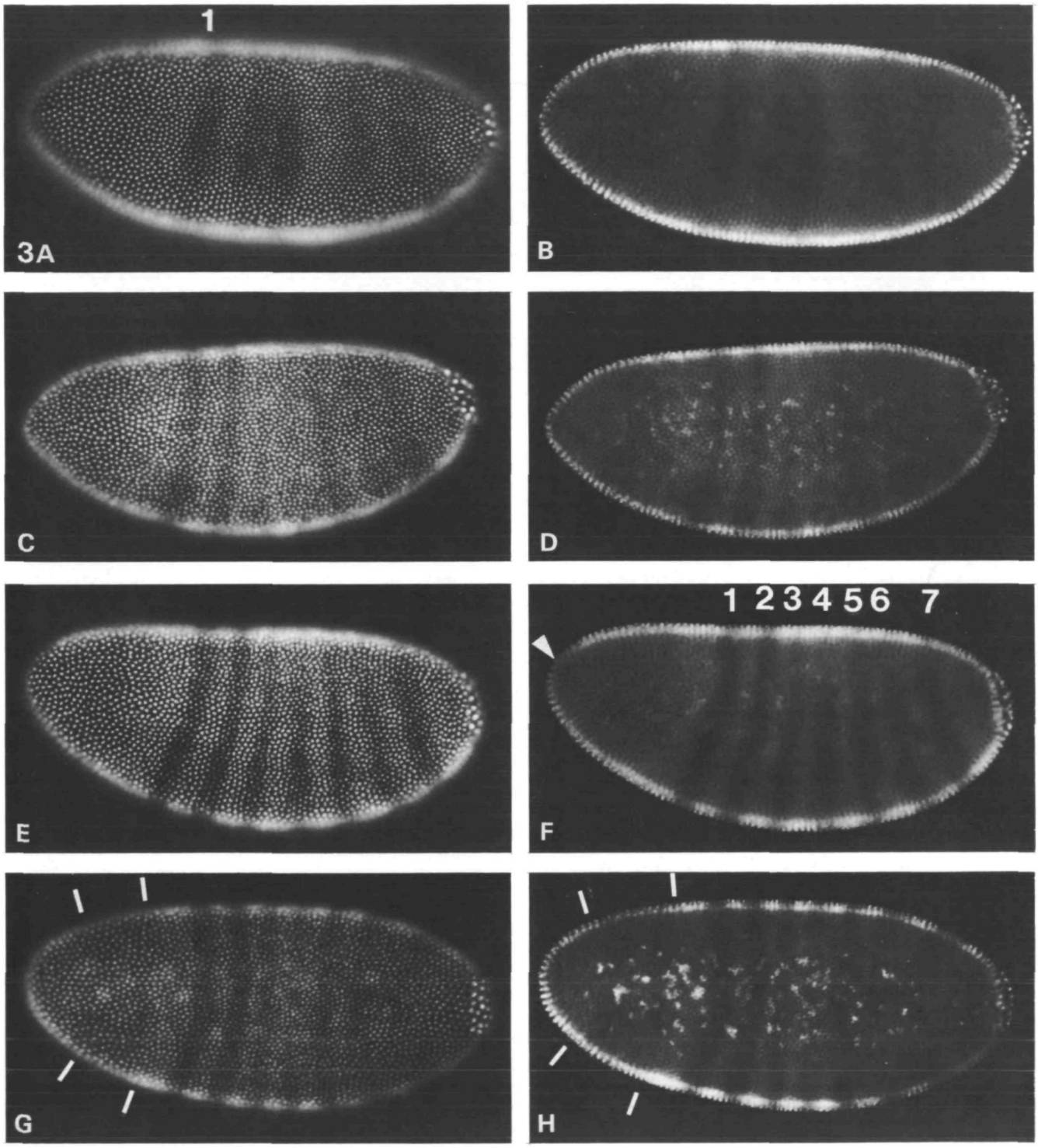

Fig. 3. *ftz* expression in cellularizing embryos – FFI visualization (see text). Focal planes are at the surface (A,C,E,G), and the middle (B,D,F,H) of the same four embryos shown in Fig. 2. The expected position of the seven major stripes are numbered in panel F, and the position of the first detectable stripe, stripe 1, is labelled in panel A. The arrowhead in F points to *ftz*-positive at the anterior tip of the embryo, and the bars in G and H denote the limits of an additional broad band of *ftz* expression anterior to stripe 1.

example, stripe 1 in Fig. 4 is approximately six nuclei wide in the region indicated by brackets, but the equivalent region in a mature cellular blastoderm pattern is approximately three to four nuclei wide (Carroll & Scott, 1985; Fig. 1). Similarly, stripes 6 and 7 together arise from *ftz* expression in a region approximately 15 nuclei wide (arrows in Fig. 4).

These initially wide bands of expression were

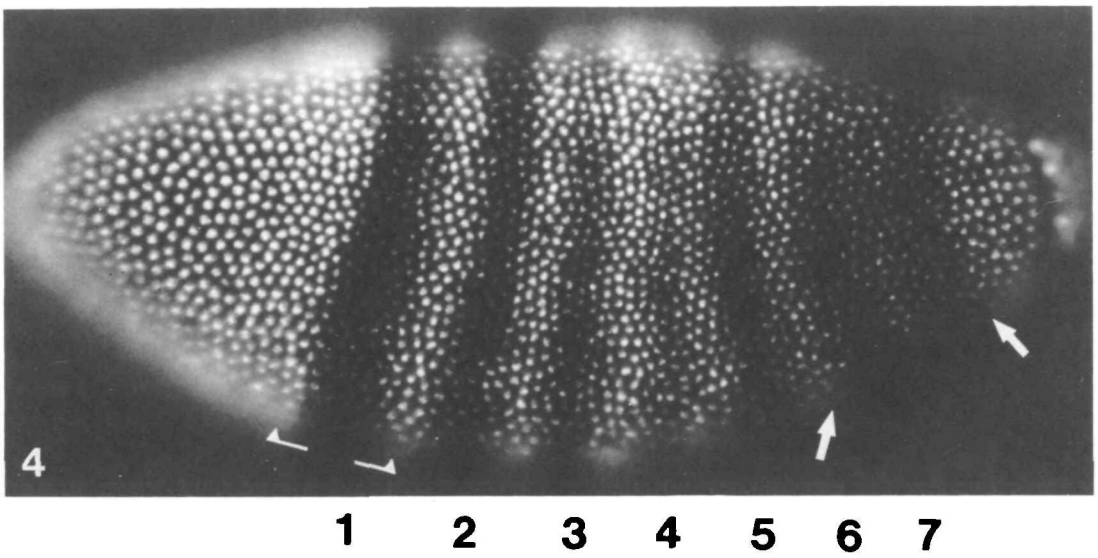

Fig. 4. Ventrolateral surface view of intermediate *ftz* patterns in an embryo fixed during cellularization and visualized by FFI. The expected position of stripes 1–7 are numbered. Brackets at the anterior end denote the extent of expression in stripe 1, and arrows point to a broad region of *ftz* expression that spans stripes 6 and 7 near the posterior end.

unevenly spaced relative to the more even spacing observed in the mature pattern. For example, the interband region between stripes 1 and 2 was initially wider than the interband region between stripes 2 and 3 (Fig. 3A,B). The spacing between stripes became more uniform as cellularization proceeded (compare Fig. 3A,B with E,F).

FFI imaging reveals new domains of ftz *protein accumulation*

In addition to the previously observed regions of *ftz* protein synthesis in stripes 1 to 7, *ftz* protein was also present in both the anterior and posterior portions of the embryo. At the anterior end, it was observed in two distinct locations: at the extreme anterior tip (Fig. 3F), and in a wide band approximately 12 nuclei wide at 75–84 % EL (Figs 1C,F; 3G,H). At the posterior end, a band of staining was present in the nuclei adjacent to the pole cells (Fig. 1C,F).

ftz protein was also detected transiently in the interband regions. An example of interband expression between stripes 6 and 7 is shown in Fig. 4. Careful inspection of embryos with intermediate *ftz* patterns revealed transient, but weak, interband expression between all of the stripes. Loss of interband expression paralleled the polarized A/P stripe formation discussed above. For example, in the embryo displayed in Fig. 4, the staining intensity of the interband between stripes 6 and 7 was greater than that between stripes 1 and 2. Thus, stripes 6 and 7 had not yet resolved into their mature pattern in this embryo.

Discussion

Enhanced immunocytochemical detection using filtered fluorescence imaging

We have found filtered fluorescence imaging (FFI) to be a sensitive and useful technique for immunohistochemical studies of nuclear antigens. FFI increases the sensitivity of the standard HRP assay. Through FFI, signal enhancement is achieved by using a fluorescent reporter group (in this case DAPI) to monitor, indirectly, a HRP-localized antigen.

In the HRP assay, antigen is detected when peroxidase activity, localized to the antigen by specific antibody binding, forms a brownish-red precipitate from 3,3′-diaminobenzidine. Unless high levels of antigen are present, the brownish signal formed has low image contrast, reducing sensitivity (see Fig. 2A). Light scattering also diminishes contrast when thick biological specimens are viewed using transmitted light. This is especially true at higher magnifications (see Fig. 2). FFI overcomes these limitations.

With epifluorescence optics and appropriate filter systems, the specimen is illuminated from above and only light from fluorescent molecules is visualized. This optical design increases sensitivity by reducing background and increasing contrast. Bright nuclear fluorescence affords high contrast and allows small local decreases in the fluorescent signal to be monitored easily by comparison with adjacent nuclei. The result is a negative image in which regions of diminished nuclear fluorescence represent the presence of antigen.

The physical basis for FFI is most likely the absorption of incident and/or fluorescent light by the HRP reaction product. In effect, the coloured HRP reaction product filters the light, thereby reducing the local density of exciting photons. As demonstrated here, FFI is useful with antigens such as *ftz* that are located in the nucleus. FFI can also be used for analysis of cytoplasmic antigens, for instance to examine antigens located between the DAPI-stained nucleus and the plane of observation (data not shown).

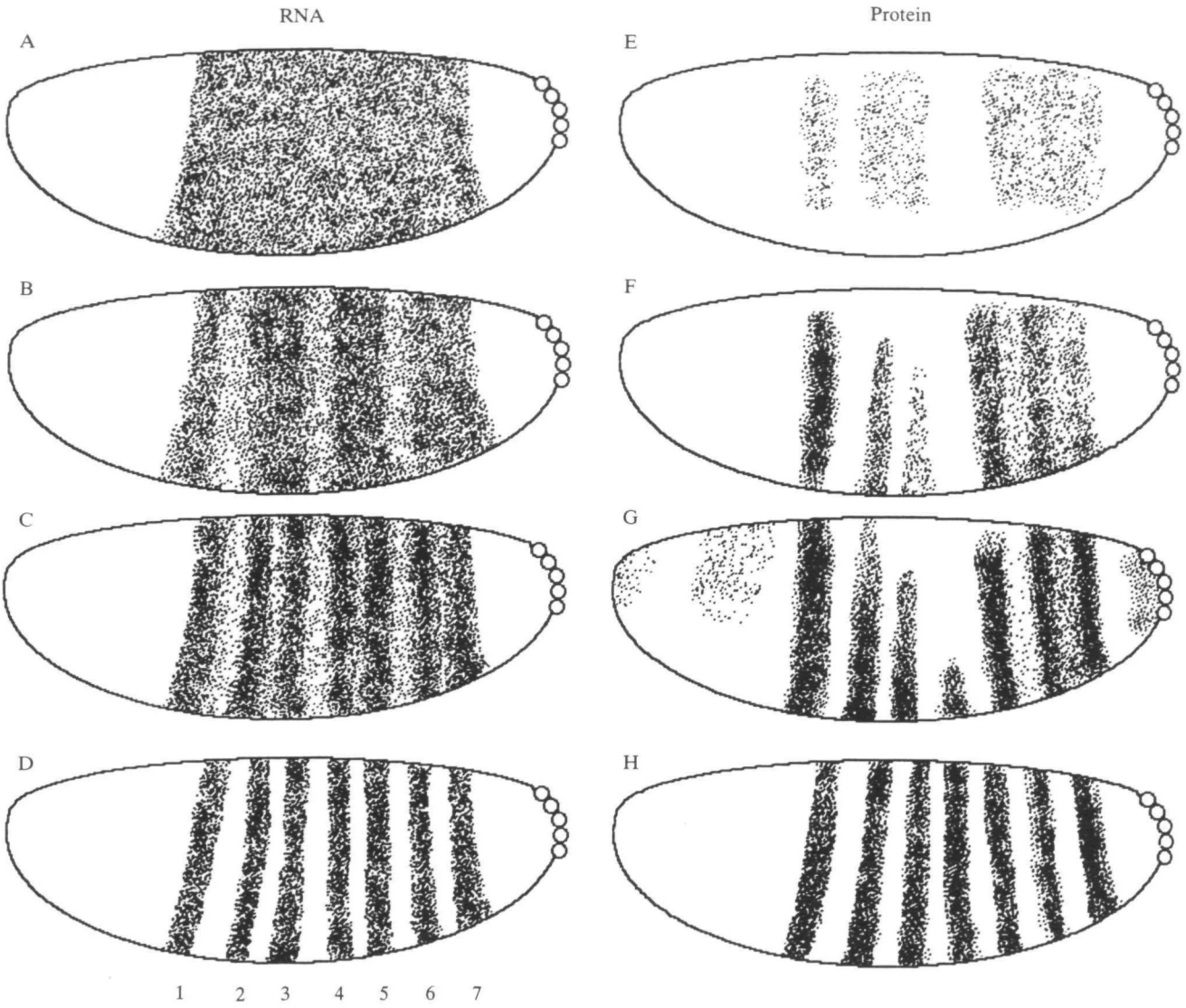

Fig. 5. Diagrammatic representation of emerging *ftz* RNA (A,B,C,D), and *ftz* protein (E,F,G,H) patterns as they would appear during the first 30 min of cellularization during cycle 14. These idealized patterns are projections onto a mid-lateral section and serve to highlight similarities and differences in the two expression patterns. Correlations between the spatial and temporal expression patterns based on previously reported RNA data (see text) and our present results suggested the alignment shown (i.e. A with E, B with F, etc.) but should be taken only as approximations. Anterior–posterior and dorsal–ventral polarities in the protein patterns are depicted by dot density.

Domains of ftz *expression*

Carroll & Scott (1985) detected *ftz* protein in seven circumferential stripes in cellular blastoderm embryos, a pattern that closely parallels the patterns of *ftz* transcripts. However, protein was not detected in younger embryos in which *ftz* RNA has been found to be more broadly distributed (Hafen *et al.* 1984; Weir & Kornberg, 1985; Ingham *et al.* 1985). Since the methods for visualizing patterns of protein and RNA were different – indirect immunofluorescence in whole-mount specimens using anti-*ftz* antibodies and RNA *in situ* hybridization to tissue sections, respectively – it is not possible to compare their relative sensitivities. Therefore, interpretation of apparent differences in spatial patterning is problematic.

However, given that in cycle-14 embryos FFI can detect *ftz* protein in regions where it had previously been undetected by either indirect immunofluorescence or RNA hybridization, it is reasonable to conclude that FFI is the more sensitive assay. Since FFI failed to detect *ftz* protein in younger embryos in which *ftz* transcripts are present in distinct patterns and at significant levels, we suggest that translation regulation limits synthesis of *ftz* protein prior to cellularization.

FFI also revealed that a low level of *ftz* protein is present in early cycle 14 embryos in many nuclei that do

not later contribute to the seven major stripes. We distinguish two aspects of these patterns. First, the broad anterior region of *ftz* protein that had not been detected with standard immunohistochemical techniques had been previously observed by two different methods. Hiromi *et al.* (1985), using *lacZ/ftz* fusion constructs, found that deletion of 5′ upstream regulatory elements resulted in additional stripes of b-galactosidase expression anterior to the cephalic furrow at the same approximate position as the broad anterior stripe detected by FFI. Also, patterns of *ftz* RNA in embryos that had been injected with cycloheximide included anterior stripes in this region. We suggest that *ftz* expression forms these anterior stripes during normal embryogenesis, albeit at a relatively low level. Second, when stripes first appear, they are not only wider than in their mature form, but also are unevenly spaced. FFI revealed that as they matured, they focused, becoming narrower and more evenly spaced. These changes are presumably due to decreased *ftz* expression in the interband regions. Given the known general transcriptional activation during cellularization, this observation raises the possibility that *ftz* is first globally activated, and then is subsequently patterned by one or more superimposed systems of repression. This interpretation is consistent with studies of cycloheximide-injected embryos in which either *ftz* expression throughout the embryo, interband expression, or additional anterior and posterior stripes of *ftz* expression were observed (Edgar *et al.* 1986). The similarity of these patterns of RNA and the patterns of protein observed by FFI suggest that cycloheximide stabilizes already existing transcripts.

Are intermediate patterns important for segmentation?

Why is *ftz* expressed in a complex pattern at low levels in cells outside of the major stripes? One possibility is that these expressing cells that do not constitute the stripes require, transiently, low levels of the *ftz* gene product, and the complex patterns of intermediate expression reflect this requirement. Alternatively, the weak expression observed outside of the major stripes could be below threshold for effective *ftz* activity, and is either vestigial or a by-product of the patterning mechanism that evolved to generate the mature stripe pattern. There is at present no evidence for a requirement for *ftz* activity in the regions outside the domains of the mature pattern. Indeed, *ftz* expression outside of the normal domains has been shown to be deleterious. For example, reciprocal pattern deletions form in embryos in which the *ftz* gene is expressed adventitiously under the control of a heat shock promoter (Struhl, 1985). Likewise, the dominant *ftz* regulatory mutations, ftz^{Rpl} and ftz^{Ual}, affect pattern elements that are out of phase with pattern deletions in *ftz* mutant embryos (Duncan, 1986). To explain the action of these dominant *ftz* alleles, broader domains of *ftz* expression were postulated (Duncan, 1986). These patterns might be similar to the transient patterns we observe in the wild-type using FFI, and it is possible that ftz^{RPL} and ftz^{Ual} mutants elevate these levels above a critical threshold.

The apparent paradox, that low levels of *ftz* protein are normally found in regions where its presence can be deleterious, might be resolved by postulating that *ftz* protein in these regions is either normally below a critical threshold for activity, or transient expression serves other (as yet unknown) functions in the patterning process. It has been proposed that patterning of the segmentation genes involves cross-regulatory interactions of the segmentation genes (Harding *et al.* 1986; Howard & Ingham, 1986; Duncan, 1986; Scott & O'Farrell, 1986; Akam, 1987; Scott & Carroll, 1987). We suggest that such patterning may require the overlapping transient expression of these proteins in the interband regions as a prerequisite for subsequent more refined spatial restrictions.

Consistent with these observations on *ftz* expression, two other pair-rule genes, *even-skipped* (Frasch *et al.* 1987) and *hairy* (Carroll *et al.* 1988), also display complex intermediate patterns during the initial stages of their expression. In addition, we have recently observed that the product of another segmentation gene, *engrailed*, also displays intermediate expression patterns outside its 14-striped domain that characterizes its mature pattern (Karr *et al.* 1989). It is possible that other segmentation genes are also expressed in complex intermediate patterns, and that these intermediates are crucial to a patterning process that involves many cross-regulatory interactions. The increased sensitivity of FFI may provide a useful tool for studying such interactions.

We wish to thank Sean Carroll, Ian Duncan, Rick Horowitz and Dave Kranz for taking time to critically read the manuscript. Very special thanks goes to Drs Steve Poole and Saul Zackson for their stylistic and editorial contributions.

References

Akam, M. (1987). The molecular basis for metameric pattern in the *Drosophila* embryo. *Development* **101**, 1–22.

Carroll, S. B., Laughon, A. & Thalley, B. S. (1988). Expression, function and regulation of the *hairy* segmentation protein in the Drosophila embryo. *Genes & Dev.* **2**, 883–890.

Carroll, S. B. & Scott, M. P. (1985). Localization of the *fushi tarazu* protein during Drosophila embryogenesis. *Cell* **43**, 47–57.

DiNardo, S., Kuner, J. M., Theis, J. & O'Farrell, P. H. (1985). Development of embryonic pattern in D. melanogaster as revealed by accumulation of the nuclear *engrailed* protein. *Cell* **43**, 59–69.

Duncan, I. M. (1986). Control of bithorax complex functions by the segmentation gene *fushi tarazu* of Drosophila melanogaster. *Cell* **47**, 297–309.

Edgar, B. A., Weir, M. P., Schubiger, G. & Kornberg, T. (1986). Repression and turnover pattern *fushi tarazu* RNA in the early Drosophila embryo. *Cell* **47**, 747–754.

Foe, V. E. & Alberts, B. (1983). Studies of nuclear and cytoplasmic behavior during the five mitotic cycles that precede gastrulation in *Drosophila* embryogenesis. *J. Cell Sci.* **61**, 31–70.

Frasch, M., Hoey, T., Rushlow, C., Doyle, H. & Levine, M. (1987). Characterization and localization of the even-skipped protein of Drosophila. *EMBO J.* **6**, 749–759.

Fullilove, S. L. & Jacobson, A. G. (1971). Nuclear elongation and cytokinesis in *Drosophila montana*. *Devl Biol.* **26**, 560–577.

Hafen, E., Kuroiwa, A. & Gehring, W. J. (1984). Spatial distribution of transcripts from the segmentation gene fushi

tarazu during Drosophila embryonic development. *Cell* **37**, 833–841.

HARDING, K., RUSHLOW, C., DOYLE, H. J., HOEY, T. & LEVINE, M. (1986). Cross-regulatory interactions among pair-rule genes in Drosophila. *Science* **233**, 953–959.

HIROMI, Y., KUROIWA, A. & GEHRING, W. J. (1985). Control elements of the Drosophila segmentation gene *fushi tarazu*. *Cell* **43**, 603–613.

HOWARD, K. & INGHAM, P. (1986). Regulatory interactions between the segmentation genes fushi tarazu, hairy, and engrailed in the Drosophila blastoderm. *Cell* **44**, 949–957.

INGHAM, P. A., HOWARD, K. R. & ISH-HOROWICZ, D. (1985). Transcription pattern of the Drosophila segmentation gene hairy. *Nature, Lond.* **318**, 439–445.

KARR, T. L. & ALBERTS, B. (1986). Organization of the cytoskeleton in early Drosophila embryos. *J. Cell Biol.* **102**, 1494–1509.

KARR, T. L., WEIR, M. D., ALI, Z. & KORNBERG, T. (1989). Patterns of engrailed protein in early Drosophila embryos. *Development* (in press).

MITCHISON, T. J. & SEDAT, J. (1983). Localization of antigenic determinants in whole Drosophila embryos. *Devl Biol.* **99**, 261–264.

NÜSSLEIN-VOLHARD, C. & WIESCHAUS, E. (1980). Mutations affecting segment number and polarity in *Drosophila. Nature, Lond.* **287**, 795–801.

SCOTT, M. P. & CARROLL, S. B. (1987). The segmentation and homeotic gene network in early Drosophila development. *Cell* **51**, 689–698.

SCOTT, M. P. & O'FARRELL, P. H. (1986). Spatial programming of gene expression in early Drosophila embryogenesis. *A. Rev. Cell Biol.* **2**, 49–80.

STRUHL, G. (1985). Near reciprocal phenotypes caused by activation or indiscriminate expression of the *Drosophila* segmentation gene *ftz*. *Nature, Lond.* **318**, 677–680.

WAKIMOTO, B. T. & KAUFMAN, T. C. (1981). Analysis of larval segmentation in lethal genotypes associated with the Antennapedia gene complex in Drosophila melanogaster. *Devl Biol.* **81**, 51–64.

WEIR, M. P. & KORNBERG, T. (1985). Patterns of engrailed and fushi tarazu transcripts reveal novel intermediate stages in *Drosophila* segmentation. *Nature, Lond.* **318**, 433–439.

(*Accepted 19 December 1988*)